

Using Enhanced Sampling Simulations to Study the Conformational Space of Chiral Aromatic Peptoid Monomers

Rakshit Kumar Jain, Carol K. Hall, and Erik E. Santiso*



Cite This: J. Chem. Theory Comput. 2023, 19, 9457-9467



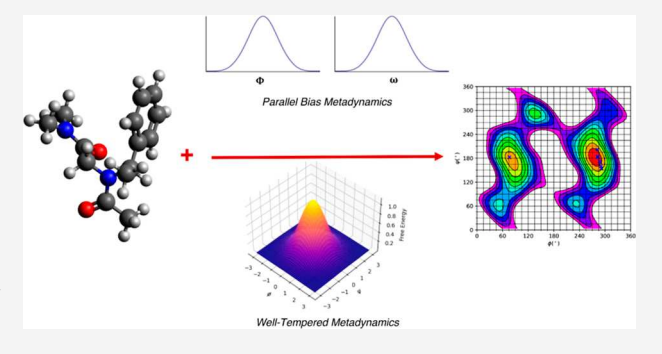
ACCESS I

Metrics & More

Article Recommendations

Supporting Information

ABSTRACT: Peptoids, or N-substituted glycines, are peptide-like materials that form a wide variety of secondary structures owing to their enhanced flexibility and a diverse collection of possible side chains. Compared to that of peptides, peptoids have a substantially more complex conformational landscape. This is mainly due to the ability of the peptoid amide bond to exist in both *cis*- and *trans*-conformations. This makes conventional molecular dynamics simulations and even some enhanced sampling approaches unable to sample the complete energy landscapes. In this article, we present an extension to the CGenFF-NTOID peptoid atomistic forcefield by adding parameters for four side chains to the previously available collection. We employ explicit solvent well-tempered metadynamics



simulations to optimize our forcefield parameters and parallel bias metadynamics to study the *cis-trans* isomerism for S_N1 -phenylethyl (s1pe) and S_N1 -naphthylethyl (s1ne) peptoid monomers, the free energy minima generated from which are validated with available experimental data. In the absence of experimental data, we supported our atomistic simulations with *ab initio* calculations. This work represents an important step toward the computational design of peptoid-based materials.

1. INTRODUCTION

Peptoids, or N-substituted glycines, are peptidomimetics that have gained huge significance in recent years due to their wide scope of application as highly tunable foldamers. 1-6 Unlike peptides, in which the residue-defining side chains are attached to the α -carbon, peptoids have their side chains attached to the backbone nitrogen atoms, making the α -carbon achiral. Thus, their stereochemistry is determined by the residue bonded to the N-atom.⁷⁻⁹ For peptides, the secondary structures are mainly governed by backbone hydrogen bonding, which allows them to adopt conformations such as polyproline-type α -helices and β sheets.^{2,3,10} In contrast, peptoid backbones are not capable of hydrogen bonding; therefore, their secondary structures are controlled by residue-specific interactions, the most common being steric effects due to the side chain size. 2,6,9 Based on the molecular structure of the side chains, inter-residue hydrogen bonding and $n \to \pi^*$ interactions (prevalent for aromatic side chains) can also influence the peptoid secondary structure. 11,12

Most peptoid molecules have a large accessible conformational space compared to that of peptides. This is because of the higher flexibility seen in the peptoid ω dihedral (Figure 1), which controls the cis—trans isomerism. Like peptides, the other important peptoid dihedrals contributing to the larger conformational landscape are ϕ and ψ dihedrals. Another important dihedral is χ , which controls the side chain planarity with the backbone. The many possible combinations of these dihedrals vastly expand the conformations for any peptoid chain.

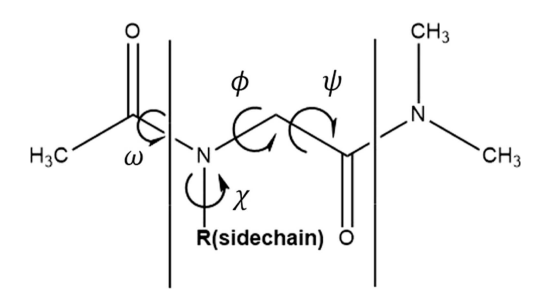


Figure 1. Peptoid monomer that we studied through our simulations. "R" represents the location where the side chains are placed. The four major peptoid dihedrals to be considered are ω , ϕ , ψ , and χ .

Since peptoid secondary structures are strongly dependent on steric interactions, their native backbone configurations are resistant to changes in external conditions such as temperature and pH.^{14,15} Peptoid secondary structures are fundamentally different from those of peptides, with the major minima being displaced by 180° with respect to the ϕ and ψ dihedral angles mentioned above, as shown in Figure 2. For this reason, peptoids

Published: November 8, 2023





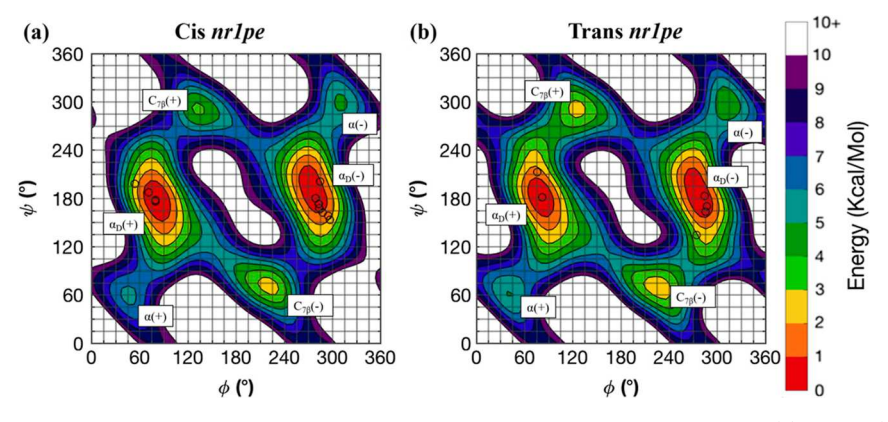


Figure 2. The major local minima states available for any peptoid are $\alpha_D \pm$, $\alpha \pm$, and $C_{7\beta} \pm$, accessible for both the (a) *cis*- and (b) *trans*-isomers as shown above in the free energy surface of *r1pe* (Figure 3b). Reproduced with permission from ref 48. Copyright 2019 John Wiley and Sons.

are also resistant to protease action as they do not fit into protease-binding pockets, which are usually tuned specifically to peptides. 16,17 The folding properties and the secondary structure expressed by a peptoid polymer can be controlled by altering the conditions during manufacturing. 2,8,10,18 Experiments have also shown that peptoids have enhanced cellular uptake properties while maintaining reduced immune responses, unlike most peptidomimetics. 19,20 All of these features make peptoid attractive candidates for investigation using both experimental and computational means. Potential applications of peptoids as curative and preventative medicine and intracellular drug delivery vehicles rely heavily on these properties.²¹⁻²⁶ Peptoids are well suited for a wide variety of material discovery applications such as antimicrobial and antifungal coatings, ^{21,26-31} energy transfer or storage sysand mimics of biologically occurring materials. These uses, along with the ease of synthesizing them using the submonomer synthesis method,³⁵ make them one of the most promising biomolecules currently being investigated.

Experiments have been instrumental in studying the influence of side chain chirality and aromaticity on peptoid-folding behavior. 10,11,36 Peptoids with achiral nonaromatic side chains such as sarcosine form helices with no turn direction preference when dissolved in polar solvents. 7,37 Most chiral peptoids that form helices display helix turn preference based on the side chain chirality, with S-side chains displaying a left-handed helix and Rside chains displaying a right-handed helix. Since peptoid secondary structures are often governed by steric forces, bulky aromatic substituents have higher helical-forming preferences than those of aliphatic side chains. 11,36 As is the case with most peptidomimetics, peptoids have the capability of forming secondary structures similar to those of peptides. The most common ones include polyproline type I (PPI) helices and parallel/antiparallel β -sheets. 8,40,41 Precise control of residue location during synthesis allows peptoids to exhibit unique secondary structures 42-44 as well as replicate the ones prevalent in peptides.

There have been several attempts to accurately describe peptoids through computational approaches. ^{13,45,46} Initial attempts used computationally expensive quantum mechanical *ab initio* approaches to optimize backbone dihedral angles for peptoid monomers/dimers. ^{13,47} In those calculations, the peptoids predominantly exhibit polyproline-type helices with the global torsional minima $\pm \alpha_D$ near $(\phi, \psi) = (\pm 75, 180^\circ)$ (Figure 2). A recent study also related these minima to the turn of the helices formed by peptoids, where $+\alpha_D$ corresponds to a

left-handed helix and $-\alpha_{\rm D}$ corresponds to the right-handed helix.³⁸ The other major minima seen in peptoids, the $C_{7\beta}$, center around $(\phi,\psi)=(120^{\circ},-75^{\circ})$ and its mirror image $(\phi,\psi)=(-120^{\circ},75^{\circ})$ (Figure 2). Since the major peptoid minima lie near the edges of a conventional Ramachandran plot, peptoid Ramachandran plots are usually displaced in both the ϕ and ψ axes by 180°, as shown in Figure 2.

Previous all-atom computational approaches to study peptoids were based on peptide forcefields like AMBER⁴⁸ and CHARMM, 46 which had limited success in predicting peptoid secondary structures. General-purpose forcefields such as GAFF⁴⁹ and OPLS⁵⁰ also had difficulties in analyzing the peptoid-cis conformations since the new parameters developed for these forcefields were only fitted to the peptoid-trans conformations. This led to refitting parameters in conventional forcefields, especially AMBER and CHARMM22, to better represent peptoid secondary structures and experimental observations. In particular, the Molecular Foundry Peptoid (MFTOID) forcefield was developed by partial refitting of the CHARMM22 parameters to reproduce the structural properties of a disarcosine peptoid molecule.⁵¹ This parameterization led to overstabilization of the trans-minima. Since the parameters were fitted to the sarcosine residue, the issue of transferring parameters between different side chains remains unresolved.

More recently, a peptoid all-atom forcefield was developed by Weiser and Santiso, who adjusted the CHARMM General ForceField (CGenFF)^{52,53} to generate parameters for the peptoid nitrogen and introduced a new atom type, NTOID.⁵⁴ They fitted all of the dihedral and improper parameters for the peptoid nitrogen, resulting in good agreement with experimentally observed structural conformations for the peptoids studied. They showed that the CGenFF-NTOID forcefield is able to correctly predict the secondary structures and major free energy minima of both the cis- and the trans-forms of two peptoid side chains, sarcosine and 1-phenylmethyl glycine. For the chiral side chain R_N1-phenylethyl glycine, CGenFF-NTOID was able to reproduce the helix-forming capability but was not able to predict the handedness expressed by the helix (Figure 2), indicating the need for further improvement of parameters developed for chiral side chains.

Recently, studies have also analyzed the formation of secondary structures in peptoid oligomers with aromatic sidechains. Molecular Dynamics simulations on *s1pe* and *r1pe* oligomers confirmed their left-handed and right handed helix structure, respectively. S5 Another study was able to determine the entropic and enthalpic contributions to folding of 12-mer

chiral peptoid oligomers, providing insight into competing forces responsible for peptoid secondary structures.⁵⁶

In this work, we extend the CGenFF-NTOID atomistic framework by fitting parameters for additional aromatic chiral side chains and predicting their *cis/trans* backbone isomerism through enhanced sampling simulations. We begin by readjusting the forcefield partial charges on S_N1-phenylethyl (Figure 3a) to obtain a better agreement with its experimentally

Figure 3. Aromatic side chain residues we studied in this paper. (a) S_N1 -phenylethyl (s1pe), (b) R_N1 -phenylethyl (r1pe), (c) S_N1 -naphthylethyl (s1ne), and (d) R_N1 -naphthylethyl (r1ne).

predicted helix-forming preferences than we had observed in our previous work. 54 We also add two new side chains, S_N and R_N 1-naphthylethyl glycine (Figure 3c,d), to our atomistic peptoid model. Well-tempered metadynamics (WTMetaD) $^{57-59}$ simulations were used to show that our parameters are invariant with the side chain R-S optical isomerism. We also perform parallel bias metadynamics (PBMetaD) 60,61 simulations to look at CGenFF-NTOID's treatment of *cis*- and *trans*-isomers and study their relative stabilities. This atomistic forcefield gives us the opportunity to study the effects of side chain chirality, aromaticity, and steric interactions on secondary structures exhibited by peptoid polymers.

In the following sections, we first present our parameter prediction and adjustment methodology, followed by details of our WTMetaD and PBMetaD simulations and a brief overview of these enhanced sampling methods. This is followed by a description of the results for WTMetaD of acetonitrile-solvated peptoid monomers before and after parameter fine-tuning for the S-side chains. PBMetaD is used to obtain the relative stabilities of all of the local peptoid minima, which show agreement with experimental observations. We also compared the results from the two enhanced sampling methodologies to see the difference in the backbone dihedral space sampled using them. We conclude by performing WTMetaD simulations for the R-side chains, comparing the free energy minima obtained with potential energy results from ab initio calculations.

2. METHODS

Peptoids have unusually high energy transition barriers between various minima for each dihedral. For instance, the transition potential energy barrier for the ω dihedral, which controls the cis—trans isomerism, is usually larger than 10 kcal/mol. For another backbone dihedral, ϕ , this barrier often fluctuates around 8–10 kcal/mol. These dihedrals and the associated barriers make accessing the complete peptoid energy landscape a tough task for most simulation techniques. To overcome these barriers, we utilize WTMetaD and PBMetaD enhanced sampling techniques with molecular dynamics, the details of which are provided in Section 2.2.

2.1. Development and Optimization of Parameters for 1-Naphthylethyl Glycine (1ne) and 1-Phenylethyl Glycine (1pe) Side Chains. The 1-naphthylethyl glycine side chain is one of the bulkiest side chains studied in experiments, and the helical propensity of cis-S_N1-naphthylethyl glycine (cissn1ne) is well documented. 42,62,63 Our initial parameters, for atom types specific to 1-naphthylethyl, were generated using ParamChem, 64 an open-source web utility developed to estimate parameters for the CGenFF forcefield. The cross-interaction parameters for NTOID with atom types not previously included in CGenFF-NTOID (such as angle and dihedral parameters involving atom types for the extended aromatic ring, additional information is provided in Supporting Information Section I) were taken from the NG2SO (proline nitrogen) atom type. 65 This was done to maintain consistency with the existing CGenFF-NTOID architecture.

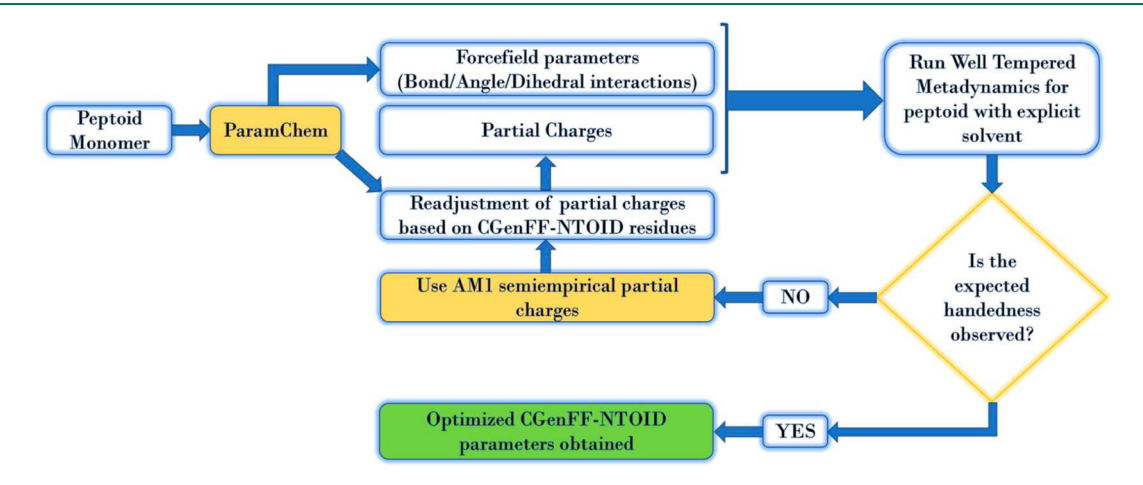


Figure 4. Partial charge and forcefield parameter optimization methods used to add side chains to the CGenFF-NTOID peptoid forcefield. The initial values generated from ParamChem are subjected to a verification algorithm and adjusted to obtain consistency with experiments.

The initial partial charges were also generated from the ParamChem utility using the peptoid monomer shown in Figure 1. Since the terminal residues of the peptoid monomer are already incorporated in CGenFF-NTOID, 34 adjustments were made to the partial charges to ensure consistency with the previously included residues so that each residue is neutral on its own. This allows us to use these developed parameters in conjunction with the already-fitted residues and perform simulations of peptoid hetero-oligomers.

CGenFF partial charges are generally constructed using the Austin model 1 (AM1) semiempirical method. 66,67 We also performed an AM1 optimization using Gaussian09⁶⁸ to get a second set of partial charges to ensure we get a better representation of the peptoid secondary structure. Like the ones generated from ParamChem, these partial charges were also adjusted to preserve agreement with the existing terminal groups from NTOID. Our partial charge and parameter optimization protocols are summarized in Figure 4. Further information on the partial charges obtained after each step of optimization and the alterations made is provided in Supporting Information, Section I.

A similar partial charge optimization protocol was also used for the *sn1pe* side chain. As reported in a previous paper, initial attempts to develop parameters for the *sn1pe* residue were not able to predict the helix turn directions for *sn1pe* monomers based on free energy calculations via explicit solvent simulations. ^{54,69} In this work, those partial charges have been modified using the algorithm represented in Figure 4 to get better agreement with experiments.

2.2. Enhanced Sampling with Metadynamics and Simulation Details. We used enhanced sampling techniques along with molecular dynamics in our simulations to ensure complete sampling of the free energy landscape. Particularly, we used two methods, WTMetaD⁵⁸ and PBMetaD,⁶⁰ which allow peptoid monomers to overcome the high transition barriers between different conformations, mainly along the ϕ , ψ , and ω dihedrals. A brief explanation of these methods is provided below.

For a system with N collective variables, WTMetaD uses an N-dimensional Gaussian biasing potential to improve sampling for the collective variables within a molecular dynamics simulation. The added potential is modified such that the Gaussian height decreases with time to ensure that the algorithm terminates once the simulation reaches convergence. So Since the biasing potential is an N-dimensional Gaussian curve, the efficiency for WTMetaD decreases exponentially with the value of N. This leads to long runtimes of WTMetaD-enhanced simulations, even for as few as 3 collective variables.

PBMetaD is a modified MetaD approach that allows efficient enhanced sampling with more than 2 collective variables. Instead of an *N*-dimensional potential as in WTMetaD, PBMetaD uses *N* 1-dimensional potentials for a system with *N* collective variables. Even though the reweighting process for PBMetaD is more mathematically involved, it makes the simulation significantly faster for a large *N*. A comparison between WTMetaD and PBMetaD can be seen in Figure 5, where the initial structure before biasing of the *sn1pe* monomer is compared with one of the resulting biased structures. A typical construction of the biasing potentials for both MetaD techniques is also shown through a pictorial representation of the added potentials in Figure 5.

Due to the aforementioned simulation runtime constraints, our choice of the enhanced sampling technique is based on the

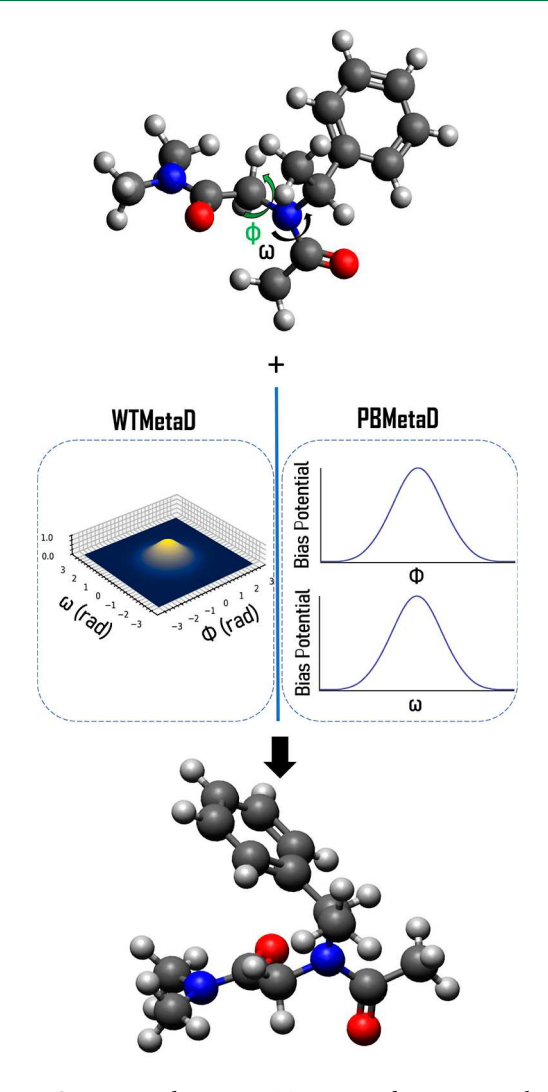


Figure 5. Comparison between WTMetaD and PBMetaD, where we show the biasing of ω and ϕ dihedrals. WTMetaD uses a 2D Gaussian biasing potential, whereas PBMetaD employs 2 1-D Gaussian biases, with the resulting biased structures being effectively identical.

number of collective variables. For simulations with only two collective variables (ϕ and ψ), we used WTMetaD, whereas for the cases with three collective variables (ϕ , ψ , and ω), we applied PBMetaD. The simulation details for both the enhanced sampling techniques are provided in Supporting Information Section II.

In our simulations, we looked at the peptoid monomer shown in Figure 1. Experiments have shown that peptoids are highly soluble in organic polar solvents such as acetonitrile and methanol. Therefore, using the software package Packmol, we solvate the molecule in acetonitrile at 298 K and 1 bar in a 40 Å \times 40 Å \times 40 Å box. The initial structure is then allowed to relax for 10 ns in the *NPT* ensemble at this temperature and pressure.

Using these solvated setups, we ran multiple WTMetaD simulations starting from the 6 local minima states applicable to peptidomimetic molecules, $\pm \alpha_{\rm D}$, $\pm \alpha$, and $\pm C_{7\beta}$ (Figure 2). In the WTMetaD setup, we biased the ϕ and ψ angles (Figure 1) as this allows us to create modified Ramachandran-like plots for peptoids where the ϕ and ψ dihedrals are displaced by 180°. After running for approximately 100 ns, the free energy histograms from each of the 6 different initial configurations were averaged together to obtain smoother free energy surfaces

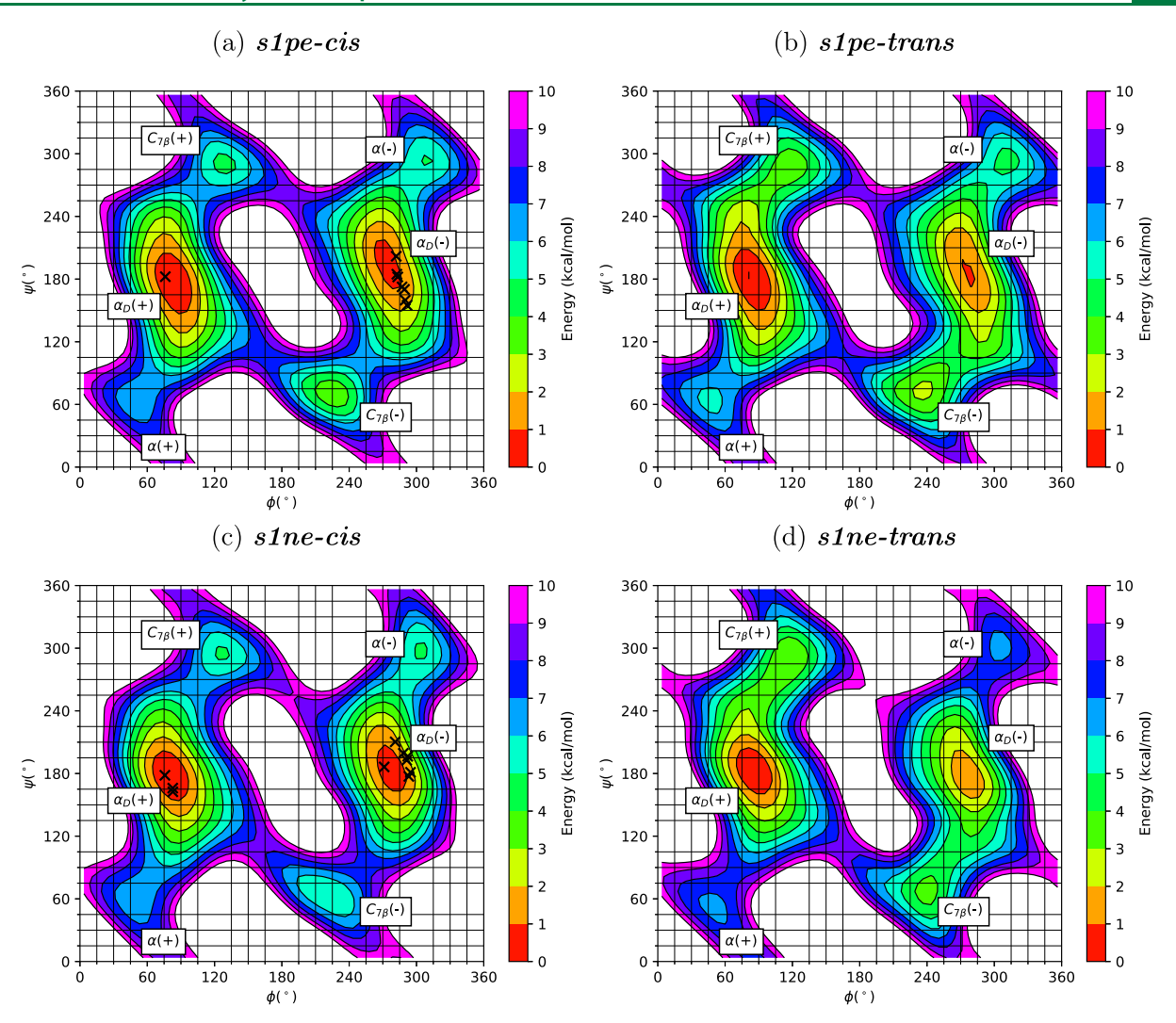


Figure 6. Original free energy surfaces generated from the partial charges taken from ParamChem for (a) S_N 1-phenylethyl *cis* form, (b) S_N 1-phenylethyl *trans* form, (c) S_N 1-naphthylethyl *cis* form, and (d) S_N 1-naphthylethyl *trans* form. The FESs are calculated after taking the average from 6 different simulations. The black "x"s represent experimental data points where the ϕ and ψ dihedrals for the stable conformations were reported. 62,69

(FESs). These plots form our initial results and help us optimize the CGenFF-NTOID forcefield parameters. We also confirmed the chiral invariance of the optimized parameters by employing WTMetaD using the same parameters and partial charges for the side chains with *R*-chirality, where we were able to observe the expected global minima through our simulations.

To compare the relative free energies of all the 12 probable metastable states for the S-side chains (cis- and trans- $\pm \alpha_{\rm D}$, $\pm \alpha$, and $\pm C_{7\beta}$), we performed PBMetaD simulations where we biased the ϕ , ψ , and ω dihedrals (Figure 1). This enables simultaneous sampling of the cis- and trans-minima states, along with the different $\phi-\psi$ conformations. This helps us confirm that the global minima predictions for the backbone dihedral free energy coincide, irrespective of the backbone cis-trans isomerism of the initial state. The three different initial state runs for both peptoid monomers are averaged after the simulation is run for 200 ns. Additional information about these calculations and the comparison between results from WTMetaD and PBMetaD is presented in Supporting Information Section IV.

3. RESULTS AND DISCUSSION

Using the WTMetaD enhanced sampling simulation methodology described in Section 2.2, we generated FESs for the S_N

isomer of the 1-phenylethyl and 1-naphthylethyl side chains using both the unadjusted partial charges obtained from the ParamChem utility (Figure 6) and the optimized partial charges obtained through the AM1 method (Figure 7). From the available experimental peptoid literature, we know that the Speptoid isomers with chiral side chains form left-handed polyproline type I (PPI) helices, and for the stable configurations, the backbone dihedrals lie around $\phi=285^\circ$ and $\psi=180^\circ$, corresponding to the $-\alpha_{\rm D}$ position on the FES. 3,13,62,69 Experimental observations involving the formation and crystallization of these peptoid oligomers further show that for S_N 1-phenylethyl and S_N 1-naphthylethyl, the cis-isomer is the stable configuration when the oligomer is solvated in acetonitrile.

Figure 6 shows the FES for S_N1 -phenylethyl and S_N1 -naphthylethyl generated using WTMetaD with the initial parameters and partial charges obtained from ParamChem before refinement. As mentioned in Section 2.2, separate WTMetaD simulations were performed for the *cis*- and *trans*-isomers of the side chains starting from 6 different configurations. Since the side chains are chiral, we expect the FES to be asymmetric around $(\phi, \psi) = (180^{\circ}, 180^{\circ})$. This is also referred to as point asymmetry and is visible in our FES. An

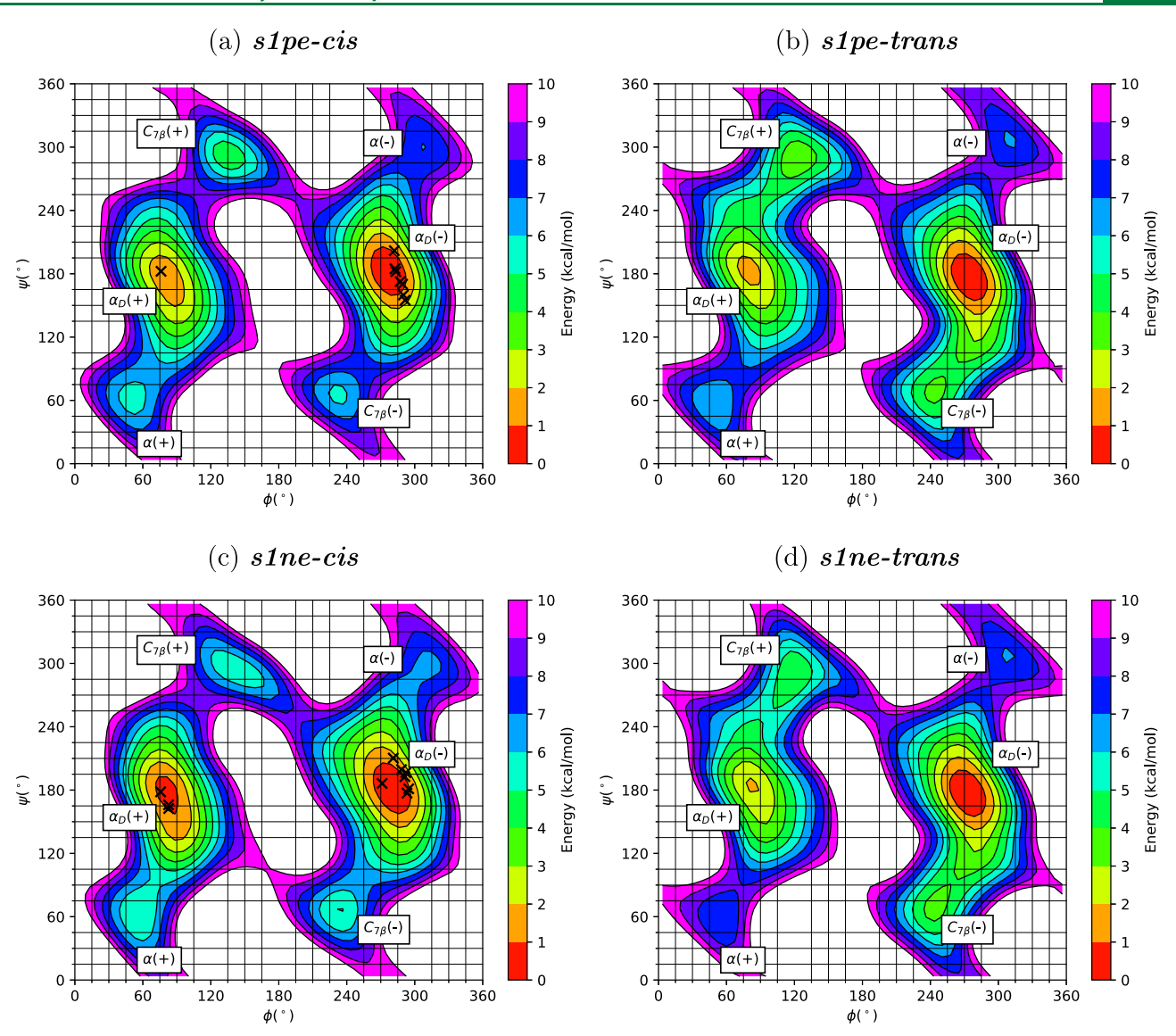


Figure 7. FESs generated after adjusting the charges according to the method detailed in Section 2.1 for (a) S_N 1-phenylethyl cis form, (b) S_N 1-phenylethyl trans form, (c) S_N 1-naphthylethyl cis form, and (d) S_N 1-naphthylethyl trans form. The FESs are calculated after taking the average from 6 different simulations. The black "x"s represent experimental data points where the ϕ and ψ dihedrals for the stable conformations were reported.

easier way to visualize it is to look at the free energies of the major minima, as none of the '+' minima have the same free energy as their '-' counterparts. These chiral aromatic peptoid side chains prefer to form PPI-type helices in their secondary structures, which is also observed in our simulations since the major minima for both the cis- and trans-isomers lie around \pm $\alpha_{\rm D}$. As mentioned earlier, experimental predictions for the cisisomer of these side chains show that the global minima should lie at $-\alpha_D$. From Figure 6, we get the free energy difference (Δ FE) between the two major minima for cis-s1pe, Δ FE_{cis-s1pe} = 0.61 ± 0.04 kcal/mol, and for cis-s1ne, $\Delta FE_{cis-s1ne} = 0.38 \pm 0.09$ kcal/mol, with $+\alpha_D$ being the global minima. Therefore, it is clear that the parameters with unadjusted charges do not give the correct helical preference, and there is no noticeable difference in the free energy values of the two major minima ($-\alpha_D$ and $+\alpha_{\rm D}$) for the *cis*-forms of both the residues.

In order to improve our prediction of the relative stabilities of the metastable states predicted for these chiral aromatic side chains, we adjusted the partial charges on the residue containing each side chain using the algorithm shown in Figure 4. Implementing the same algorithm for WTMetaD using these new partial charges, as detailed in Section 2.2, led to the FES for both the *cis*- and *trans*-isomers of the two side chains *s1pe* and *s1ne* shown in Figure 7. As intended, the new partial charges do not significantly change the location of the free energy minima but can adjust their relative stability. This partial charge adjustment gave the correct handedness prediction for the *cis*-form, where the experimental observations tell us that the global minima should be at $-\alpha_{\rm D}$. Furthermore, Δ FE along ψ = 180° for *cis-s1pe* is Δ FE_{*cis-s1pe*} = 1.34 \pm 0.09 kcal/mol and for *cis-s1ne* is Δ FE_{*cis-s1ne*} = 0.84 \pm 0.10 kcal/mol, with the $-\alpha_{\rm D}$ state as the global minima. This makes us confident that the new parameters and partial charges can accurately predict the most stable secondary structures for these peptoid residues.

We also employed PBMetaD simulations with the newly fitted partial charges to study the relative stability of all of the local minima of the S_N 1-phenylethyl glycine and S_N 1-naphthylethyl glycine peptoid monomers. As mentioned in Section 2.2, we biased three dihedrals, ϕ , ψ , and ω , for each side chain and performed three runs with different initial states to calculate free

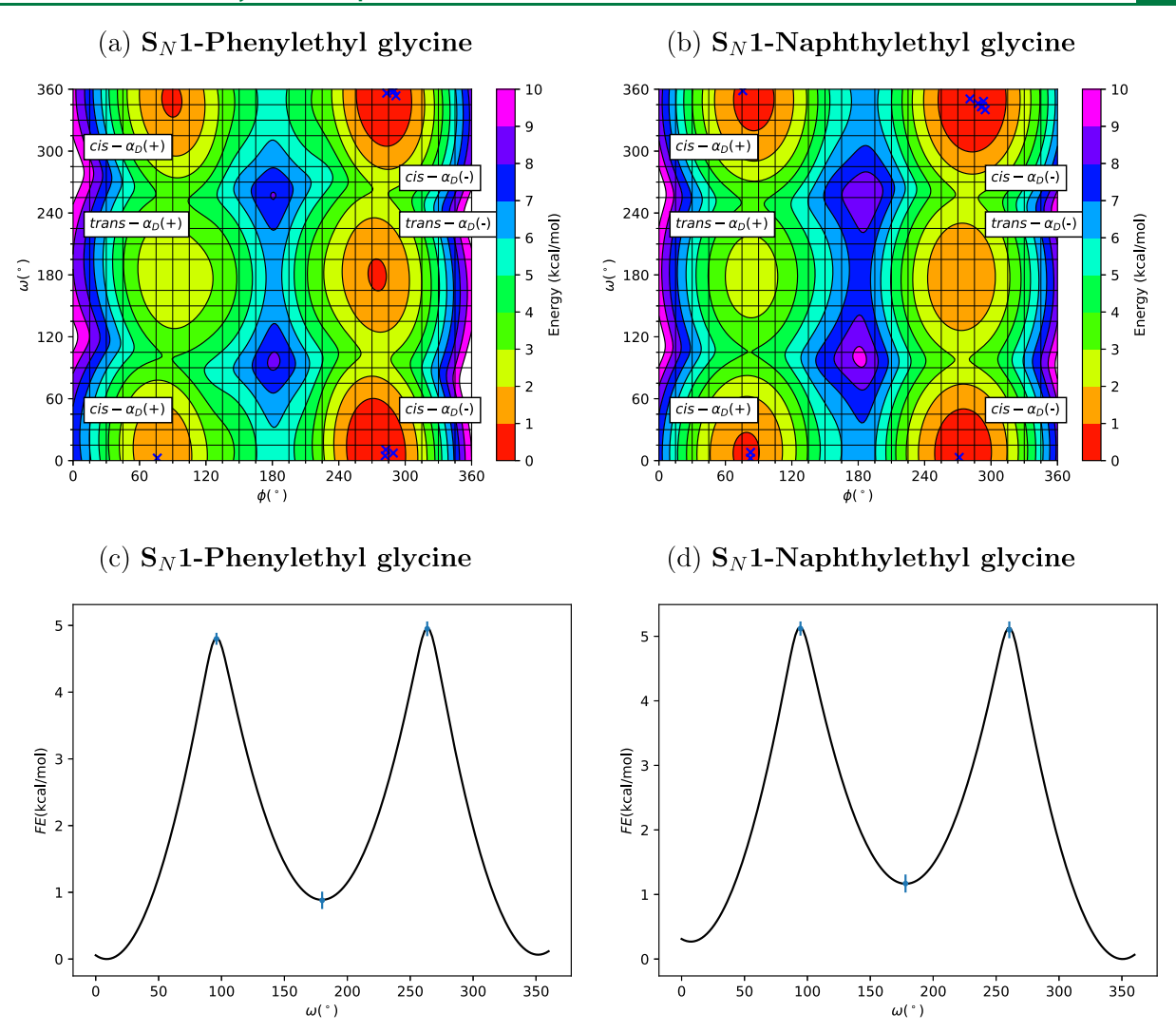


Figure 8. $\phi-\omega$ FESs generated using PBMetaD for (a) S_N1 -phenylethyl glycine and (b) S_N1 -naphthylethyl glycine. The blue "x"s represent experimental data points where the ϕ and ω dihedrals for the stable conformations were reported. ^{62,69} Also shown are 1-D free energy profiles for (c) S_N1 -phenylethyl and (d) S_N1 -naphthylethyl side chains generated from PBMetaD simulations. The error bars (blue lines) in (c,d) are the RMSE from three simulations starting with different initial configurations.

energies. These were then averaged to improve the smoothness of the results, as shown in Figure 8. Before averaging, the average free energy difference between the runs with the three different initial states was less than 0.3 kcal/mol, which makes us confident that the simulations have converged. As we expected, the PBMetaD simulations are in good agreement with the WTMetaD computations, which can be seen by comparing the $\phi-\psi$ Ramachandran plots (Supporting Information Section IV). After reweighing the biased simulations to remove the effect of the added Gaussian potential, we were also able to generate ϕ - ω FES for both the peptoid monomers, snlpe and snlne, shown in Figure 8a,b, respectively. The lowest free energy configurations observed in our PBMetaD simulations for s1pe correspond to $(\phi, \omega) = (273.5^{\circ}, 8.04^{\circ})$, and for the s1ne monomer, they correspond to $(\phi, \omega) = (283.5^{\circ}, 349.94^{\circ})$. This matches experimental observations that the most stable state is $cis-\alpha_D(-)$. These FESs also inform us of a possible cis-trans transformation route, where the free energy barrier of least height is seen along $\phi = 283^{\circ}$ (Figure 8a,b). The PBMetaD simulations predict an isomerization-free energy barrier of 5.12 \pm 0.11 kcal/mol for the s1ne monomer and 4.80 \pm 0.09 kcal/mol for the slpe peptoid monomer. The slightly higher barrier for sIne is due to the larger size of the naphthyl substituent in the s1ne monomer, which increases the steric hindrance between the side chain and backbone, thereby restricting its motion. It is important to note that this barrier is likely an underestimation as most experimental observations tell us that this barrier is usually ~10 kcal/mol. CGenFF-NTOID was made such that this barrier remains low to enable efficient transitions between the cis- and trans-isomers for the different side chains. Barrier underestimation notwithstanding, this is an important starting point for researchers interested in studying peptoid cis-trans isomerism as it informs us of the most probable path these peptoid side chains take during the cis-trans transition. Furthermore, from Figure 8c,d, we can deduce that the free energy difference between the cis- and trans-isomers for slpe is 0.88 ± 0.13 kcal/ mol, whereas for slne, this difference is $1.17 \pm 0.14 \text{ kcal/mol}$, with the cis-form being more stable. This is also consistent with experimentally observed values of the global peptoid minima.^{62,69}

In order to confirm the invariance of these parameters for optical isomers, we also generate FES for the R_N isomers of both the peptoid monomers, i.e., R_N 1-phenylethyl glycine (Figure 3b) and R_N 1-naphthylethyl glycine (Figure 3d). Even though

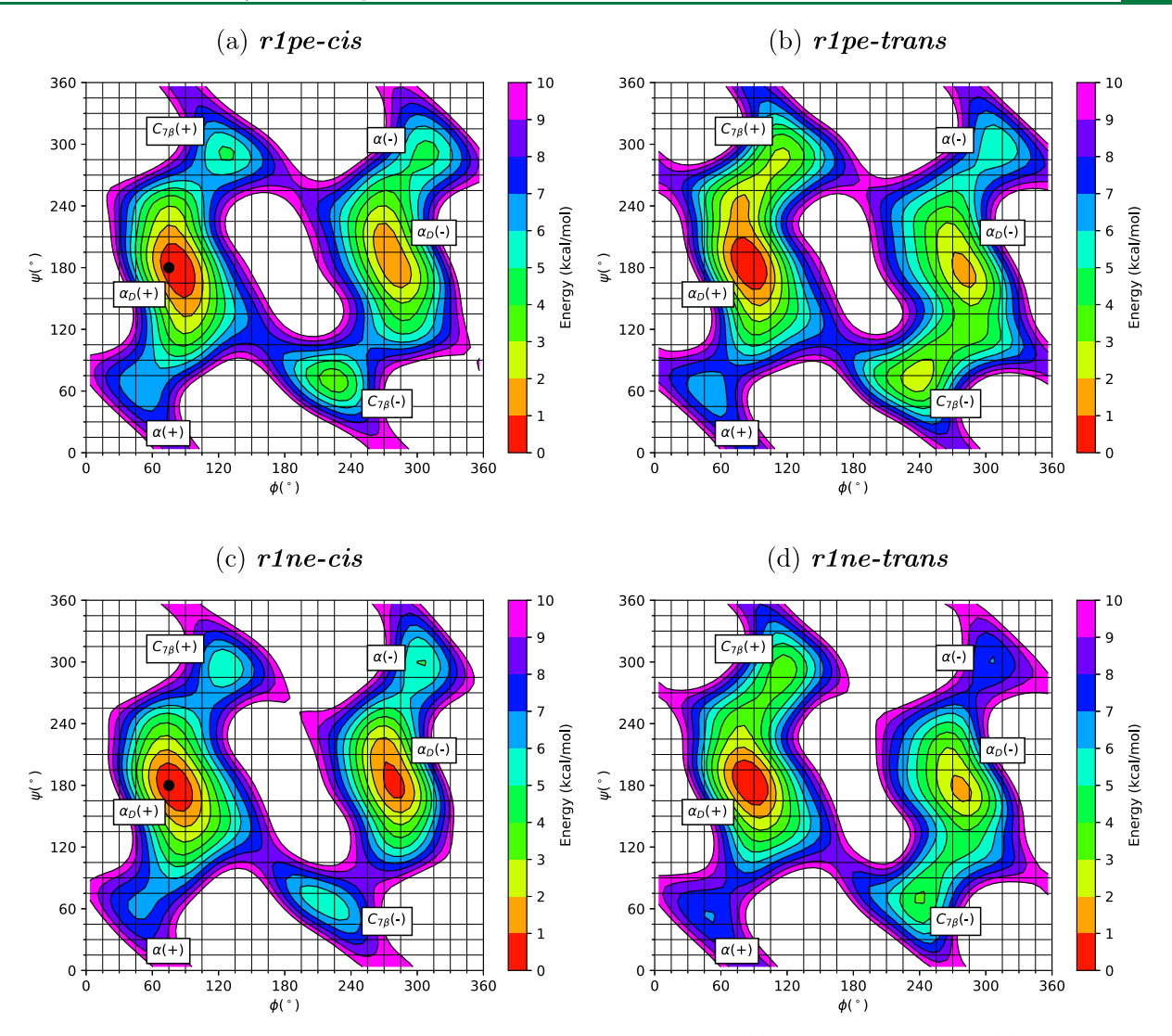


Figure 9. FESs generated from altered charges but the same parameters as used in Figure 7 for (a) R_N1 -phenylethyl *cis* form, (b) R_N1 -phenylethyl *trans* form, (c) R_N1 -naphthylethyl *cis* form, and (d) R_N1 -naphthylethyl *trans* form. The black filled circle represents the lowest potential energy configuration observed through MP2/6-31G* *ab initio* computations.

there is a lack of experimental structural predictions for these isomers, there is consensus among experimentalists that these R_N isomers should form helices that exhibit the opposite handedness than their S_N forms. This is reproduced in our FESs, which show the global minima centered around the $+\alpha_D$ state, i.e., $\phi = 75^\circ$ and $\psi = 180^\circ$ for the *cis*-form (Figure 9).

As a means to further validate our predictions for the R_N isomers, we also performed ab initio calculations using Gaussian09. Here, we started with the two major minima $(\pm \alpha_D)$ and let the monomer relax at the MP2/6-31G* level of theory, in concurrence with most peptoid computations performed at the ab initio scale. After the initial relaxation, we calculated the single-point potential energy for the monomer at the same level of theory. These simulations are performed in triplicates and averaged to give the potential energy (Table 1). According to these calculations, the lowest potential energy isomer for both of the peptoid monomers was predicted to be close to cis- $\alpha_D(-)$, which corresponds with our free energy calculations. Furthermore, the relative ordering of the local minima predicted by WTMetaD is in agreement with the results obtained through ab initio calculations for both r1pe and r1ne.

Table 1. Potential Energy Values for R_N 1-Phenylethyl Glycine (r1pe) and R_N 1-Naphthylethyl Glycine (r1ne) Calculated from Ab Initio Simulations Using the MP2/6-31G* Basis Set^a

peptoid monomer	φ (°)	ψ (°)	minima name	potential energy (kcal/mol)	free energy (kcal/mol)
r1pe-cis	75	180	cis - $lpha_{ m D}$ +	-3.78 ± 0.02	-4.85 ± 0.15
r1pe-trans	75	180	$trans-lpha_{ m D}+$	-3.26 ± 0.005	-3.83 ± 0.15
r1pe-cis	-75	180	cis- $lpha_{ m D}$ -	-1.97 ± 0.01	-2.58 ± 0.18
r1pe-trans	-75	180	trans-	-1.71 ± 0.02	-1.25 ± 0.21
			$lpha_{ ext{D}}$ -		
r1ne-cis	75	180	cis - $lpha_{ m D}$ +	-5.86 ± 0.02	-5.07 ± 0.12
r1ne-trans	75	180	$trans-lpha_{ m D}+$	-4.96 ± 0.02	-4.82 ± 0.16
r1ne-cis	-75	180	cis- $lpha_{ m D}$ -	-1.91 ± 0.01	-4.27 ± 0.17
r1ne-trans	-75	180	trans- $lpha_{ m D}$ -	-0.45 ± 0.005	-3.35 ± 0.25

^aThe reference states for both r1pe and r1ne are set to their respective cis- $C_{7\beta}$ local minima.

4. CONCLUDING REMARKS

1-Phenylethyl glycine and 1-naphthylethyl glycine are some of the most studied peptoid side chains. They have been used for a variety of applications, ranging from biomedical uses to the development of new and improved materials. Through our simulations, we have shown that the CGenFF-NTOID forcefield coupled with WTMetaD is able to predict the global structural minima accurately. We artificially reduce the high transition barriers between various minima to maintain backbone flexibility so that the forcefield can be used for different biological and material discovery applications.

Using PBMetaD, we have been able to study the relative energies of the peptoid *cis—trans* isomers, which have been largely unexplored for peptoids to date. WTMetaD simulations have been used to verify the chiral invariance of the parameters developed in this work (Figure 9). This gives us confidence that the CGenFF-NTOID parameters developed for new chiral side chains will enable us to analyze both the optical isomers (*R*- and *S*-) using WTMetaD and PBMetaD simulations.

A pressing challenge for simulations is studying the behavior of these side chains in longer peptoid chains. Even though conventional molecular dynamics cannot completely sample the peptoid energy landscape, PBMetaD has the capability of biasing a large number of collective variables, which could overcome this limitation.

CGenFF-NTOID represents one of the first atomistic forcefields developed, especially for peptoids, that is able to accurately predict free energy minima, including the accurate sampling of both the *cis*- and *trans*-amide bond configurations. This also provides us the opportunity to obtain information available only through simulations, such as the relative heights of the free energy barriers and the free energy differences between various minima. The parameters developed for atomistic simulations will provide a much-needed step for accurate structure and binding property prediction of these peptoid side chains.

ASSOCIATED CONTENT

Supporting Information

The Supporting Information is available free of charge at http://pubs.acs.org/doi/10.1021/acs.jctc.3c00803.

NAMD files used to do PBMetaD analysis for the S-isomers for the 1-phenylethyl glycine and 1-naphthylethyl glycine side chains (ZIP)

Partial charge readjustment for peptoid monomers, simulation parameters and descriptions, chiral invariance of forcefield parameters, and PBMetaD vs WTMetaD for peptoid monomers (PDF)

AUTHOR INFORMATION

Corresponding Author

Erik E. Santiso — Department of Chemical and Biomolecular Engineering, North Carolina State University, Raleigh, North Carolina 27606, United States; orcid.org/0000-0003-1768-8414; Email: eesantis@ncsu.edu

Authors

Rakshit Kumar Jain — Department of Chemical and Biomolecular Engineering, North Carolina State University, Raleigh, North Carolina 27606, United States; orcid.org/ 0009-0000-7788-0550 Carol K. Hall – Department of Chemical and Biomolecular Engineering, North Carolina State University, Raleigh, North Carolina 27606, United States; orcid.org/0000-0002-7425-587X

Complete contact information is available at: https://pubs.acs.org/10.1021/acs.jctc.3c00803

Note

The authors declare no competing financial interest.

ACKNOWLEDGMENTS

The authors would like to acknowledge funding from NSF CSSI: ELEMENTS (OAC-1835838). We also thank Dr. Jim Pfaendtner and Dr. Sarah Alamdari for their help with the intricacies of parallel bias metadynamics.

REFERENCES

- (1) Qiu, Z.; Zhang, M.; Liu, D.; Shen, X.; Zhou, W.; Liu, W.; Lu, J.; Guo, L. A Review on the Synthesis of Polypeptoids. *Catalysts* **2023**, *13*, 280–304.
- (2) Zhang, D.; Lahasky, S. H.; Guo, L.; Lee, C.-U.; Lavan, M. Polypeptoid Materials: Current Status and Future Perspectives. *Macromolecules* **2012**, *45*, 5833–5841.
- (3) Robertson, E. J.; Battigelli, A.; Proulx, C.; Mannige, R. V.; Haxton, T. K.; Yun, L.; Whitelam, S.; Zuckermann, R. N. Design, Synthesis, Assembly, and Engineering of Peptoid Nanosheets. *Acc. Chem. Res.* **2016**, *49*, 379–389.
- (4) Sun, J.; Zuckermann, R. N. Peptoid Polymers: A Highly Designable Bioinspired Material. ACS Nano 2013, 7, 4715–4732.
- (5) Knight, A. S.; Zhou, E. Y.; Francis, M. B.; Zuckermann, R. N. Sequence Programmable Peptoid Polymers for Diverse Materials Applications. *Adv. Mater.* **2015**, *27*, 5665–5691.
- (6) Fowler, S. A.; Blackwell, H. E. Structure-function relationships in peptoids: Recent advances toward deciphering the structural requirements for biological function. *Org. Biomol. Chem.* **2009**, *7*, 1508–1524.
- (7) Yoo, B.; Kirshenbaum, K. Peptoid architectures: elaboration, actuation, and application. *Curr. Opin. Chem. Bio.* **2008**, *12*, 714–721.
- (8) Zuckermann, R. N. Peptoid origins. *Pept. Sci.* **2011**, *96*, 545–555.
- (9) Luxenhofer, R.; Fetsch, C.; Grossmann, A. Polypeptoids: A perfect match for molecular definition and macromolecular engineering? *J. Polym. Sci., Part A: Polym. Chem.* **2013**, *51*, 2731–2752.
- (10) Shin, H.-M.; Kang, C.-M.; Yoon, M.-H.; Seo, J. Peptoid helicity modulation: precise control of peptoid secondary structures via position-specific placement of chiral monomers. *Chem. Commun.* **2014**, *50*, 4465–4468.
- (11) Wu, C.; Sanborn, T.; Huang, K.; Zuckermann, R.; Barron, A. Peptoid oligomers with alpha-chiral, aromatic side chains: Sequence requirements for the formation of stable peptoid helices. *J. Am. Chem. Soc.* **2001**, *123*, *6778*–*6784*.
- (12) Gorske, B. C.; Nelson, R. C.; Bowden, Z. S.; Kufe, T. A.; Childs, A. M. "Bridged" $n\rightarrow\pi^*$ Interactions Can Stabilize Peptoid Helices. *J. Org. Chem.* **2013**, 78, 11172–11183.
- (13) Butterfoss, G. L.; Renfrew, P. D.; Kuhlman, B.; Kirshenbaum, K.; Bonneau, R. A Preliminary Survey of the Peptoid Folding Landscape. *J. Am. Chem. Soc.* **2009**, *131*, 16798–16807.
- (14) Schunk, H. C.; Austin, M. J.; Taha, B. Z.; McClellan, M. S.; Suggs, L. J.; Rosales, A. M. Oxidative degradation of sequence-defined peptoid oligomers. *Mol. Syst. Des. Eng.* **2023**, *8*, 92–104.
- (15) Perez Bakovic, G. R.; Roberts, J. L.; Colford, B.; Joyce, M.; Servoss, S. L. Peptoid microsphere coatings: The effects of helicity, temperature, pH, and ionic strength. *Biopolymers* **2019**, *110*, No. e23283.
- (16) Miller, S.; Simon, R.; Ng, S.; Zuckermann, R.; Kerr, J.; Moos, W. Comparison of the Proteolytic Susceptibilities of Homologous Lamino-acid, D-amino-acid, and N-substituted Glycine Peptide and Peptoid Oligomers. *Drug Dev. Res.* **1995**, *35*, 20–32.

- (17) Miller, S.; Simon, R.; Ng, S.; Zuckermann, R.; Kerr, J.; Moos, W. Proteolytic Studies of Homologous Peptide and N-substituted Glycine Peptoid Oligomers. *Bioorg. Med. Chem. Lett.* **1994**, *4*, 2657–2662.
- (18) Zborovsky, L.; Smolyakova, A.; Baskin, M.; Maayan, G. A. A Pure Polyproline Type I-like Peptoid Helix by Metal Coordination. *Chem.—Eur. J.* **2018**, *24*, 1159–1167.
- (19) Wender, P.; Mitchell, D.; Pattabiraman, K.; Pelkey, E.; Steinman, L.; Rothbard, J. The design, synthesis, and evaluation of molecules that enable or enhance cellular uptake: Peptoid molecular transporters. *Proc. Natl. Acad. Sci. U.S.A.* **2000**, *97*, 13003–13008.
- (20) Huang, W.; Seo, J.; Lin, J. S.; Barron, A. E. Peptoid transporters: effects of cationic, amphipathic structure on their cellular uptake. *Mol. BioSyst.* **2012**, *8*, 2626–2628.
- (21) Ryge, T.; Hansen, P. Novel lysine-peptoid hybrids with antibacterial properties. *J. Pept. Sci.* **2005**, *11*, 727–734.
- (22) Andreev, K.; Martynowycz, M. W.; Gidalevitz, D. Peptoid drug discovery and optimization via surface X-ray scattering. *Biopolymers* **2019**, *110*, No. e23274.
- (23) Zhang, W.; Deng, S.; Zhou, M.; Zou, J.; Xie, J.; Xiao, X.; Yuan, L.; Ji, Z.; Chen, S.; Cui, R.; et al. Host defense peptide mimicking cyclic peptoid polymers exerting strong activity against drug-resistant bacteria. *Biomater. Sci.* **2022**, *10*, 4515–4524.
- (24) Herlan, C. N.; Meschkov, A.; Schepers, U.; Bräse, S. Cyclic Peptoid-Peptide Hybrids as Versatile Molecular Transporters. *Front. Chem.* **2021**, *9*, 9.
- (25) Shukla, S. P.; Cho, K. B.; Rustagi, V.; Gao, X.; Fu, X.; Zhang, S. X.; Guo, B.; Udugamasooriya, D. G. "Molecular Masks" for ACE2 to Effectively and Safely Block SARS-CoV-2 Virus Entry. *Int. J. Mol. Sci.* **2021**, 22, 8963.
- (26) Diamond, G.; Molchanova, N.; Herlan, C.; Fortkort, J. A.; Lin, J. S.; Figgins, E.; Bopp, N.; Ryan, L. K.; Chung, D.; Adcock, R.; et al. Potent Antiviral Activity against HSV-1 and SARS-CoV-2 by Antimicrobial Peptoids. *Pharmaceuticals* **2021**, *14*, 304.
- (27) Molchanova, N.; Hansen, P. R.; Franzyk, H. Advances in Development of Antimicrobial Peptidomimetics as Potential Drugs. *Molecules* **2017**, *22*, 1430.
- (28) Corson, A. E.; Armstrong, S. A.; Wright, M. E.; McClelland, E. E.; Bicker, K. L. Discovery and Characterization of a Peptoid with Antifungal Activity against Cryptococcus neoformans. *ACS Med. Chem. Lett.* **2016**, *7*, 1139–1144.
- (29) Liu, R.; Chen, X.; Hayouka, Z.; Chakraborty, S.; Falk, S. P.; Weisblum, B.; Masters, K. S.; Gellman, S. H. Nylon-3 Polymers with Selective Antifungal Activity. *J. Am. Chem. Soc.* **2013**, *135*, 5270–5273.
- (30) Greco, I.; Hummel, B. D.; Vasir, J.; Watts, J. L.; Koch, J.; Hansen, J. E.; Nielsen, H. M.; Damborg, P.; Hansen, P. R. In Vitro ADME Properties of Two Novel Antimicrobial Peptoid-Based Compounds as Potential Agents against Canine Pyoderma. *Molecules* **2018**, 23, 630.
- (31) Wu, B. C.; Skovbakke, S. L.; Masoudi, H.; Hancock, R. E. W.; Franzyk, H. In vivoAnti-inflammatory Activity of Lipidated Peptidomimetics Pam-(Lys-beta Nspe)(6)-NH(2)and Lau-(Lys-beta Nspe)(6)-NH(2)Against PMA-Induced Acute Inflammation. *Front. Immunol.* **2020**, *11*, 11.
- (32) Kang, B.; Yang, W.; Lee, S.; Mukherjee, S.; Forstater, J.; Kim, H.; Goh, B.; Kim, T.-Y.; Voelz, V. A.; Pang, Y.; et al. Precisely tuneable energy transfer system using peptoid helix-based molecular scaffold. *Sci. Rep.* **2017**, *7*, 4786.
- (33) Yang, W.; Jo, J.; Oh, H.; Lee, H.; Chung, W.-j.; Seo, J. Peptoid Helix Displaying Flavone and Porphyrin: Synthesis and Intramolecular Energy Transfer. *J. Org. Chem.* **2020**, *85*, 1392–1400.
- (34) Huang, M. L.; Ehre, D.; Jiang, Q.; Hu, C.; Kirshenbaum, K.; Ward, M. D. Biomimetic peptoid oligomers as dual-action antifreeze agents. *Proc. Natl. Acad. Sci. U.S.A.* **2012**, *109*, 19922–19927.
- (35) Tran, H.; Gael, S. L.; Connolly, M. D.; Zuckermann, R. N. Solid-phase Submonomer Synthesis of Peptoid Polymers and their Self-Assembly into Highly-Ordered Nanosheets. *J. Visualized Exp.* **2011**, *57*, No. e3373.
- (36) Seo, J.; Barron, A. E.; Zuckermann, R. N. Novel Peptoid Building Blocks: Synthesis of Functionalized Aromatic Helix-Inducing Submonomers. *Org. Lett.* **2010**, *12*, 492–495.

- (37) Jefferson, E.; Locardi, E.; Goodman, M. Incorporation of achiral peptoid-based trimeric sequences into collagen mimetics. *J. Am. Chem. Soc.* **1998**, *120*, 7420–7428.
- (38) Spencer, R. K.; Butterfoss, G. L.; Edison, J. R.; Eastwood, J. R.; Whitelam, S.; Kirshenbaum, K.; Zuckermann, R. N. Stereochemistry of polypeptoid chain configurations. *Biopolymers* **2019**, *110*, No. e23266.
- (39) Wu, C.; Sanborn, T.; Zuckermann, R.; Barron, A. Peptoid oligomers with alpha-chiral, aromatic side chains: Effects of chain length on secondary structure. *J. Am. Chem. Soc.* **2001**, *123*, 2958–2963.
- (40) Zhao, M.; Lachowski, K. J.; Zhang, S.; Alamdari, S.; Sampath, J.; Mu, P.; Mundy, C. J.; Pfaendtner, J.; De Yoreo, J. J.; Chen, C. L.; et al. Hierarchical Self-Assembly Pathways of Peptoid Helices and Sheets. *Biomacromolecules* **2022**, *23*, 992–1008.
- (41) Robertson, E. J.; Olivier, G. K.; Qian, M.; Proulx, C.; Zuckermann, R. N.; Richmond, G. L. Assembly and molecular order of two-dimensional peptoid nanosheets through the oil-water interface. *Proc. Natl. Acad. Sci. U.S.A.* **2014**, *111*, 13284–13289.
- (42) Gorske, B. C.; Mumford, E. M.; Gerrity, C. G.; Ko, I. A Peptoid Square Helix via Synergistic Control of Backbone Dihedral Angles. *J. Am. Chem. Soc.* **2017**, *139*, 8070–8073.
- (43) Mannige, R. V.; Haxton, T. K.; Proulx, C.; Robertson, E. J.; Battigelli, A.; Butterfoss, G. L.; Zuckermann, R. N.; Whitelam, S. Peptoid nanosheets exhibit a new secondary-structure motif. *Nature* **2015**, 526, 415–420.
- (44) Crapster, J. A.; Guzei, I. A.; Blackwell, H. E. A Peptoid Ribbon Secondary Structure. *Angew. Chem., Int. Ed.* **2013**, *52*, 5079–5084.
- (45) Reese, H. R.; Shanahan, C. C.; Proulx, C.; Menegatti, S. Peptide science: A "rule model" for new generations of peptidomimetics. *Acta Biomater.* **2020**, *102*, 35–74.
- (46) J Weiser, L.; E Santiso, E. Molecular modeling studies of peptoid polymers. *AIMS Mater. Sci.* **2017**, *4*, 1029–1051.
- (47) Butterfoss, G. L.; Yoo, B.; Jaworski, J. N.; Chorny, I.; Dill, K. A.; Zuckermann, R. N.; Bonneau, R.; Kirshenbaum, K.; Voelz, V. A. De novo structure prediction and experimental characterization of folded peptoid oligomers. *Proc. Natl. Acad. Sci. U.S.A.* **2012**, *109*, 14320–14325.
- (48) Voelz, V. A.; Dill, K. A.; Chorny, I. Peptoid Conformational Free Energy landscapes From Implicit-Solvent Molecular Simulations in AMBER. *Biopolymers* **2011**, *96*, 639–650.
- (49) Mukherjee, S.; Zhou, G.; Michel, C.; Voelz, V. A. Insights into Peptoid Helix Folding Cooperativity from an Improved Backbone Potential. *J. Phys. Chem. B* **2015**, *119*, 15407–15417.
- (50) Du, P.; Rick, S. W.; Kumar, R. Towards a coarse-grained model of the peptoid backbone: the case of N,N-dimethylacetamide. *Phys. Chem. Chem. Phys.* **2018**, 20, 23386–23396.
- (51) Mirijanian, D. T.; Mannige, R. V.; Zuckermann, R. N.; Whitelam, S. Development and Use of an Atomistic CHARMM-Based Forcefield for Peptoid Simulation. *J. Comput. Chem.* **2014**, *35*, 360–370.
- (52) Vanommeslaeghe, K.; Hatcher, E.; Acharya, C.; Kundu, S.; Zhong, S.; Shim, J.; Darian, E.; Guvench, O.; Lopes, P.; Vorobyov, I.; et al. CHARMM General Force Field: A Force Field for Drug-Like Molecules Compatible with the CHARMM All-Atom Additive Biological Force Fields. *J. Comput. Chem.* **2010**, *31*, 671–690.
- (53) Yu, W.; He, X.; Vanommeslaeghe, K.; MacKerell, A. D., Jr. Extension of the CHARMM general force field to sulfonyl-containing compounds and its utility in biomolecular simulations. *J. Comput. Chem.* **2012**, 33, 2451–2468.
- (54) Weiser, L. J.; Santiso, E. E. A CGenFF-based force field for simulations of peptoids with both cis and trans peptide bonds. *J. Comput. Chem.* **2019**, *40*, 1946–1956.
- (55) Alamdari, S.; Pfaendtner, J. Origins of Conformational Heterogeneity in Peptoid Helices. *J. Phys. Chem. B* **2023**, *127* (27), 6163–6170.
- (56) Alamdari, S.; Torkelson, K.; Wang, X.; Chen, C. L.; Ferguson, A. L.; Pfaendtner, J. Thermodynamic Basis for the Stabilization of Helical Peptoids by Chiral Sidechains. *J. Phys. Chem. B* **2023**, *127* (27), 6171–6183.

- (57) Laio, A.; Gervasio, F. L. Metadynamics: a method to simulate rare events and reconstruct the free energy in biophysics, chemistry and material science. *Rep. Prog. Phys.* **2008**, *71*, 126601.
- (58) Barducci, A.; Bussi, G.; Parrinello, M. Well-tempered metadynamics: A smoothly converging and tunable free-energy method. *Phys. Rev. Lett.* **2008**, *100*, 020603.
- (59) Hosek, P.; Kriz, P.; Toulcova, D.; Spiwok, V. Multisystem altruistic metadynamics-Well-tempered variant. *J. Chem. Phys.* **2017**, *146*, 125103.
- (60) Pfaendtner, J.; Bonomi, M. Efficient Sampling of High-Dimensional Free-Energy Landscapes with Parallel Bias Metadynamics. *J. Chem. Theory Comput.* **2015**, *11*, 5062–5067.
- (61) Prakash, A.; Fu, C. D.; Bonomi, M.; Pfaendtner, J. Biasing Smarter, Not Harder, by Partitioning Collective Variables into Families in Parallel Bias Metadynamics. *J. Chem. Theory Comput.* **2018**, *14*, 4985–4990.
- (62) Stringer, J. R.; Crapster, J. A.; Guzei, I. A.; Blackwell, H. E. Extraordinarily Robust Polyproline Type I Peptoid Helices Generated via the Incorporation of alpha-Chiral Aromatic N-1-Naphthylethyl Side Chains. *J. Am. Chem. Soc.* **2011**, *133*, 15559–15567.
- (63) Gorske, B. C.; Mumford, E. M.; Conry, R. R. Tandem Incorporation of Enantiomeric Residues Engenders Discrete Peptoid Structures. *Org. Lett.* **2016**, *18*, 2780–2783.
- (64) Mackerell, Jr., A.; Vanommeslaeghe, K. ParamChem. 2010. https://cgenff.umaryland.eduweb/(accessed Oct, 2023).
- (65) Vanommeslaeghe, K.; MacKerell, A. D., Jr. Automation of the CHARMM General Force Field (CGenFF) I: Bond Perception and Atom Typing. *J. Chem. Inf. Model.* **2012**, *52*, 3144–3154.
- (66) Vanommeslaeghe, K.; Raman, E. P.; MacKerell, A. D., Jr. Automation of the CHARMM General Force Field (CGenFF) II: Assignment of Bonded Parameters and Partial Atomic Charges. *J. Chem. Inf. Model.* **2012**, *52*, 3155–3168.
- (67) Murrell, J. Semi-empirical electronic structure methods. *J. Mol. Struct.*: THEOCHEM 1998, 424, 93–99.
- (68) Frisch, M. J.; Trucks, G. W.; Schlegel, H. B.; Scuseria, G. E.; Robb, M. A.; Cheeseman, J. R.; Scalmani, G.; Barone, V.; Mennucci, B.; et al. *Gaussian09* Revision E.01; Gaussian Inc.: Wallingford CT, 2009.
- (69) Huang, K.; Wu, C.; Sanborn, T.; Patch, J.; Kirshenbaum, K.; Zuckermann, R.; Barron, A.; Radhakrishnan, I. A threaded loop conformation adopted by a family of peptoid nonamers. *J. Am. Chem. Soc.* **2006**, *128*, 1733–1738.
- (70) Martínez, L.; Andrade, R.; Birgin, E. G.; Martínez, J. M. PACKMOL: A package for building initial configurations for molecular dynamics simulations. *J. Comput. Chem.* **2009**, *30*, 2157–2164.

NOTE ADDED AFTER ASAP PUBLICATION

This paper originally published ASAP on November 8, 2023. The text in the Introduction was updated, and two new references were added in a new version that reposted on November 21, 2023.